International Journal of Nanomedicine

Dovepress
open access to scientific and medical research

Open Access Full Text Article

ORIGINAL RESEARCH

Folic acid-targeted disulfide-based cross-linking micelle for enhanced drug encapsulation stability and site-specific drug delivery against tumors

This article was published in the following Dove Press journal:
International Journal of Nanomedicine
18 March 2016
Number of times this article has been viewed

Yumin Zhang[1,*]
Junhui Zhou[2,*]
Cuihong Yang[1]
Weiwei Wang[3]
Liping Chu[1]
Fan Huang[1]
Qiang Liu[1]
Liandong Deng[2]
Deling Kong[3]
Jianfeng Liu[1]
Jinjian Liu[1]

[1]Tianjin Key Laboratory of Radiation Medicine and Molecular Nuclear Medicine, Institute of Radiation Medicine, Chinese Academy of Medical Science and Peking Union Medical College, [2]Department of Polymer Science and Technology, School of Chemical Engineering and Technology, Tianjin University, [3]Tianjin Key Laboratory of Biomaterial Research, Institute of Biomedical Engineering, Chinese Academy of Medical Science and Peking Union Medical College, Tianjin, People's Republic of China

*These authors contributed equally in this work

Correspondence: Jianfeng Liu; Jinjian Liu
Tianjin Key Laboratory of Radiation Medicine and Molecular Nuclear Medicine, Institute of Radiation Medicine, Chinese Academy of Medical Science and Peking Union Medical College, No. 238, Baidi road, Nankai district, Tianjin 300192, People's Republic of China
Email lewis78@163.com; liujinjian2002@163.com

Abstract: Although the shortcomings of small molecular antitumor drugs were efficiently improved by being entrapped into nanosized vehicles, premature drug release and insufficient tumor targeting demand innovative approaches that boost the stability and tumor responsiveness of drug-loaded nanocarriers. Here, we show the use of the core cross-linking method to generate a micelle with enhanced drug encapsulation ability and sensitivity of drug release in tumor. This kind of micelle could increase curcumin (Cur) delivery to HeLa cells in vitro and improve tumor accumulation in vivo. We designed and synthesized the core cross-linked micelle (CCM) with polyethylene glycol and folic acid-polyethylene glycol as the hydrophilic units, pyridyldisulfide as the cross-linkable and hydrophobic unit, and disulfide bond as the cross-linker. CCM showed spherical shape with a diameter of 91.2 nm by the characterization of dynamic light scattering and transmission electron microscope. Attributed to the core cross-linking, drug-loaded CCM displayed higher Nile Red or Cur-encapsulated stability and better sensitivity to glutathione than noncross-linked micelle (NCM). Cellular uptake and in vitro antitumor studies proved the enhanced endocytosis and better cytotoxicity of CCM-Cur against HeLa cells, which had a high level of glutathione. Meanwhile, the folate receptor-mediated drug delivery (FA-CCM-Cur) further enhanced the endocytosis and cytotoxicity. Ex vivo imaging studies showed that CCM-Cur and FA-CCM-Cur possessed higher tumor accumulation until 24 hours after injection. Concretely, FA-CCM-Cur exhibited the highest tumor accumulation with 1.7-fold of noncross-linked micelle Cur and 2.8-fold of free Cur. By combining cross-linking of the core with active tumor targeting of FA, we demonstrated a new and effective way to design nanocarriers for enhanced drug encapsulation, smart tumor responsiveness, and elevated tumor accumulation.

Keywords: core cross-linking, folic acid targeting, self-assembling, curcumin, drug delivery, micelles

Introduction

With the emergence and rapid development of nanocarriers for drug delivery systems in recent decades, the shortcomings of small molecule antitumor drugs, such as high side effects and low solubility, were efficiently improved. After being entrapped by various nanosized vehicles,[1–4] the circulation time of therapeutic agents was prolonged, and the concentration of drugs accumulated into tumor sites was enhanced owing to the enhanced permeability and retention effect.[5,6] However, the nanocarrier for this drug delivery system is still confronted with a series of barriers when applied to antitumor activities in vitro and in vivo.[7–9] Among them, encapsulation stability is an urgent problem to be solved. First, when drug-loaded nanocarriers are exposed to the blood stream or normal tissues, the core-shell structure of nanocarriers may be dissolved

submit your manuscript | www.dovepress.com
Dovepress
http://dx.doi.org/10.2147/IJN.S101649

and diluted to a concentration below their critical micelle concentration (CMC), which can result in a trail of side effects.[10,11] Second, conventional nanocarriers that loaded drugs by physical entrapment suffered from the premature release of drugs in systemic circulation after being injected into humans or animals. That is, up to 20%–30% of the entrapped drugs are leaked out before being delivered to the therapeutic sites, which cause off-target effects.[12]

To address this issue, the cross-linked micelle (CM) was proposed. A shell cross-linked micelle (SCM) has been previously reported and was achieved via radical oligomerization of the pendent styrenyl groups on the coronal blocks in a tetrahydrofuran–water mixture.[13–15] Structure and drug encapsulation of the SCM were more stable than noncross-linked micelle (NCM) with respect to infinite dilution in the blood circulation. Nevertheless, the drugs loaded into the SCM could not quickly release in cells; it had to follow a passive diffusion because of the nonsensitive cores of the SCM.[16–19] Meanwhile, the SCM by the preparation of a diblock copolymer was obliged to consider the intermicellar cross-linking, which might lead to micelle aggregates. The large micelle aggregates can be cleared by the mononuclear phagocyte system. Therefore, a nanocarrier with characteristics of high encapsulation and controlled drug release is forcefully required so as to improve the therapeutic efficiency in the treatment of tumors.

In most cases, some core cross-linked micelles (CCMs) were designed by different intermolecular forces between polymer chains, such as Van der Waals forces, hydrogen bonds, and hydrophobic and electrostatic interactions.[20,21] However, the stability of the micelle by the contribution of the weak noncovalent interactions is undesirable.[22] In previous reports, acid-sensitive CCM could not only load and deliver drugs more stably but also control and sustain the release of drugs by the breakage of acid-labile cross-linker in the core.[23,24]

Folate receptors are overexpressed in most types of epithelium-related cancer cells, while being almost undetectable in healthy tissues or cells.[25,26] Nanocarriers modified by folic acid (FA) can actively deliver drugs to tumors through folate receptor-mediated active targeting,[27,28] resulting in the improved therapeutic effect.[26] Meanwhile, the antitumor efficiency may be significantly strengthened by synergetic active and passive tumor targeting.[29]

Herein, we report a CCM fabricated by the self-assembly of folic acid-polyethylene glycol (FA-PEG) and pyridyldisulfide (PDS),[30,31] with polyethylene glycol (PEG) and FA-PEG as the hydrophilic units and PDS as the cross-linkable and hydrophobic unit, which was sensitive to reducing agents.[32,33] The disulfide bonds in the core of the micelle were formed by thiol-exchange reaction, and the "net structure" consisting of disulfide bonds could protect drugs from leakage into the blood circulation. When the CCM arrived at the tumor sites, the net structure in the core of micelles was destroyed by high concentrations of glutathione (GSH), and the drug loaded by CCM achieved stimuli drug release in response to high reducibility stimulus (Figure 1). In order to explore the unique characteristics of CCM in vitro and in vivo, we used Nile Red and curcumin (Cur) as the model drugs. The drug loading stability and controlled release activities of CCM were investigated in vitro. The cellular uptake and in vitro tumor cell inhibition ability were also studied. The in vivo drug delivery and tumor-targeting profiles were mainly explored by tissue distribution and tumor accumulation experiments.

Materials and methods

Materials

N-(3-(Dimethylamino)propyl)-*N*-ethylcarbodiimide hydrochloride (EDC·HCl), *N*-hydroxysuccinimide (NHS), dithiothreitol (DTT), and 2,2-azobis (isobutyronitrile) (AIBN) were purchased from Alfa Aesar (Lancashire, UK). $mPEG_{5k}$-NH_2 and FA-PEG_{5K}-NH_2 were purchased from JenKem Technology Co., Ltd. (Beijing, China). 3-(4,5-Dimethyl-2-thiazolyl)-2,5-diphenyl-2-H-tetrazolium bromide (MTT) and Cur were purchased from Sigma-Aldrich Co. (St Louis, MO, USA). Tetrahydrofuran and dimethyl formamide were provided by Jiangtian Company (Tianjin, People's Republic of China) and dried by refluxing over calcium hydride and then distilled.

Synthesis and characterizations of polymer and micelles

Chain transfer agent of *N*-(2-(2-pyridyl disulfide) ethyl methacrylamide (DS) and S-1-dodecyl-S-(α,α′-dimethyl-α″-acetic acid) trithiocarbonate (CTAm) was synthesized as reported.[34] Macro chain transfer agent of FA-PEG_{5k}-CTAm and $mPEG_{5k}$-CTAm was synthesized according to our previous work.[35] The amphiphilic block copolymers mPEG-*b*-PDS (PGDS) and FA-PEG-*b*-PDS (FPGDS) were synthesized by using $mPEG_{5k}$-CTAm and FA-PEG_{5k}-CTAm as the chain transfer agent, respectively. Briefly, $mPEG_{5k}$-CTAm (1.073 g, 0.2 mM), DS (3.048 g, 12 mM), and AIBN (6.56 mg, 0.04 mM) were dissolved in anhydrous dimethyl formamide (5 mL) in a 25 mL Schlenk flask. After degassing via three freeze–pump–thaw cycles, the flask was placed in a thermostatic oil bath at 70°C for 24 hours in atmosphere.

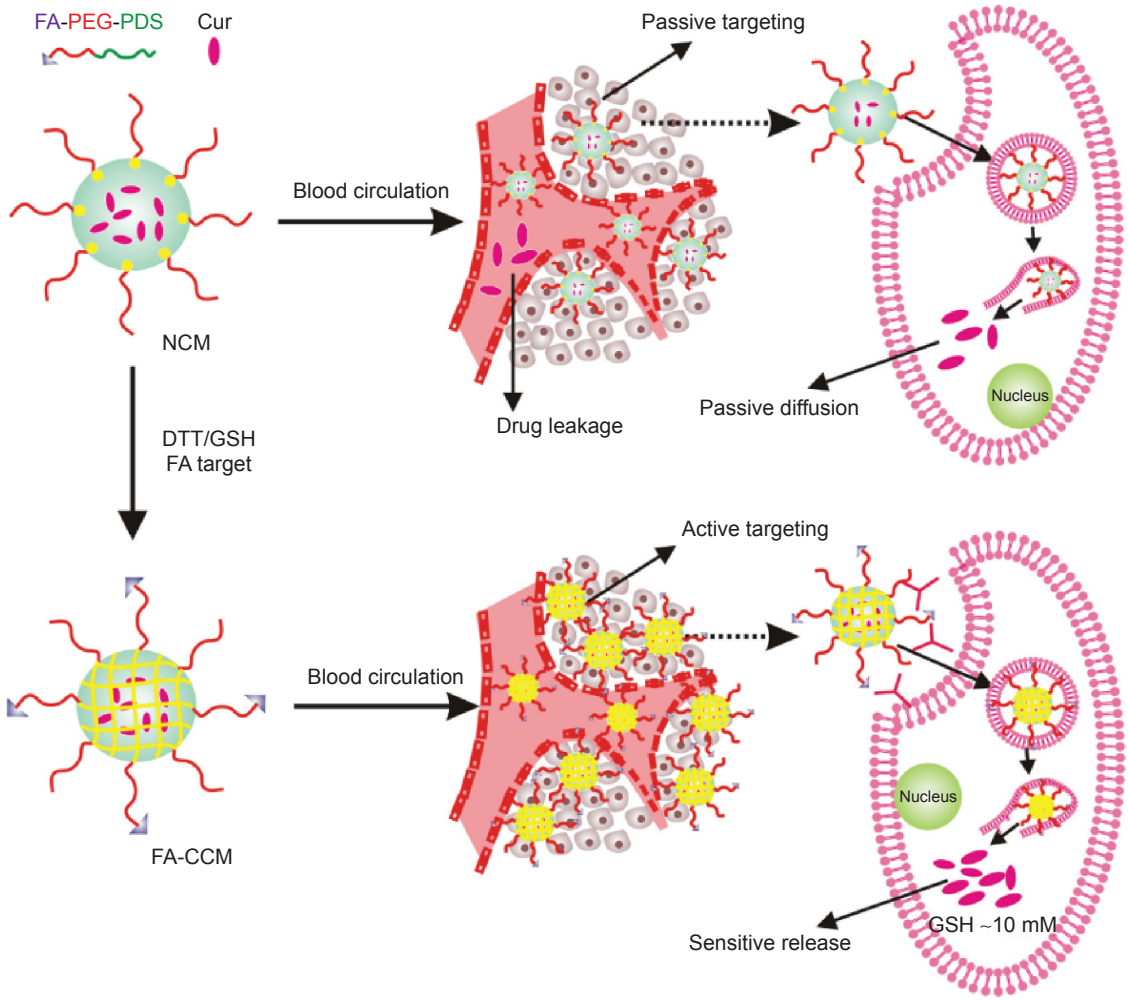

Figure 1 Illustration of different behaviors of drug delivering and releasing in vivo between NCM and FA-CCM.
Abbreviations: NCM, noncross-linked micelle; FA, folic acid; CCM, cross-linked micelle; FA-PEG, folic acid-polyethylene glycol; PDS, pyridyldisulfide; Cur, curcumin; DTT, dithiothreitol; GSH, glutathione.

Then, the solution was dialyzed against pure water for 2 days and finally lyophilized to obtain the powder of PGDS. The polymer FPGDS was synthesized via the same route. The structures and compositions of copolymers were characterized by ^{1}H NMR (solvent: $CDCl_3$) using a Varian INOVA 500 MHz NMR instrument at 25°C.

Preparation and characterization of micelles

PGDS micelle (NCM) was prepared via nanoprecipitation method. Briefly, 20 mg of PGDS copolymer was dissolved in 1 mL of dimethyl sulfoxide, and then the mixture was incubated for 20 minutes and dialyzed against phosphate-buffered saline (PBS; 0.01 M, pH 7.4) for 24 hours using a dialysis bag (molecular weight cutoff [MWCO]: 3,500 Da). Finally, the concentration of PGDS polymer in the NCM solution was adjusted to 1 mg/mL for the following experiments. To obtain the disulfide-responsive core cross-linked PGDS micelle (CCM), calculated amount of DTT (1.2 equiv of DS monomers) was added into the prepared NCM and then incubated for 24 hours, which ensured that all of the PDS units in the NCM were cross-linked. Core cross-linked FPGDS micelle (FA-CCM) was prepared through the same route. Particle size and size distribution of these micelles were determined by dynamic light scattering (Brookhaven BI-200SM) at λ=532 nm with a fixed detector angle of 173°. Morphology of the self-assembled structure was investigated using a Hitachi H600 transmission electron microscope at operated voltage of 75 kV.

Characterization of redox sensitivity of CCM

Redox sensitivity of CCM was investigated using varian fluorescence spectrophotometer (Varian, Palo Alto, USA).

Here, we chose Nile Red as fluorescent probe. Nile Red-loaded NCM (NCM-NR) and CCM (CCM-NR) were prepared, respectively. Briefly, the polymer (20 mg) was dissolved in dimethyl sulfoxide (1 mL) consisting of Nile Red (20 μg), and then the mixture was dialyzed (MWCO: 3,500 Da) against PBS (0.01 M, pH 7.4), in which DTT (1.2 equiv of DS monomers) was added to prepare the Nile Red-loaded NCM. After incubated for 24 hours, CCM-NR was obtained. NCM-NR and CCM-NR were divided into six groups, which were processed under different conditions such as various pH values and with or without GSH treated. As incubated time went by, the fluorescence values of the treated micelles solution were measured by varian fluorescence spectrophotometer.

Release of Cur in vitro

The release character of Cur from NCM-Cur and CCM-Cur was assessed by the dialysis bag methods. To obtain the drug release profile, Cur was loaded by NCM during NCM synthesis, and CCM-Cur was prepared via similar method of CCM as depicted in the method of synthesis and characterizations of polymer and micelles. Meanwhile, the FA-CCM-Cur was prepared for further studies. Briefly, 50% of PGDS and 50% of FPGDS were co-self-assembled into NCM, DTT (1.2 equiv of DS monomers) was added into the prepared NCM and then incubated for 24 hours, which ensured that all of the PDS units in the PGDS and FPGDS were cross-linked. Drug loading content (DLC) and drug loading efficiency (DLE) were calculated with the following equations:

$$\text{DLC (\%)} = \frac{\text{Weight of loaded Cur}}{\text{Weight of Cur loaded NPs}} \times 100\% \quad (1)$$

$$\text{DLE (\%)} = \frac{\text{Weight of loaded Cur}}{\text{Weight of Cur in feed}} \times 100\% \quad (2)$$

NCM-Cur (5 mL, 1.0 mg/mL) and CCM-Cur (5 mL, 1.0 mg/mL) were sealed in a dialysis bag (MWCO: 8,000 Da) and incubated in 25 mL different kinds of buffer solutions (pH 7.4 or 5.0 value, and with or without GSH treated) at 37°C under stirring at a speed of 80 rpm. 5 mL of buffer solutions was taken out and supplemented by the same volume of fresh buffer solutions at selected time intervals. The concentration of Cur in removed buffer solutions was measured by ultraviolet–visible spectrophotometry at 425 nm, and the percentages of Cur released from micelles were plotted against time. Each sample for the release kinetics study was conducted in triplicate.

Cellular uptake study

HeLa cells (human henrietta lackes strain of cancer cell line) were cultured in Dulbecco's Modified Eagle's Medium supplemented with 10% fetal bovine serum at 37°C in 5% CO_2. All cell experiments were carried out according to the People's Republic of China national standard (GB/T 16886.5-2003) and were approved by the Chinese Academy of Medical Science and Peking Union Medical College. Cells were seeded into a 12-well plate with a density of 10^5 cells/well. After incubation for 24 hours, cells were incubated with free Cur, NCM-Cur, CCM-Cur, and FA-CCM-Cur at equivalent Cur concentration of 20 μg/mL, respectively. After cultured for 8 hours, the mixture of liquids in each well was discarded and washed three times with PBS. Each well was observed using fluorescence microscopy with an excitation wavelength of 490 nm.

For flow cytometric analyses, HeLa cells were seeded onto 24-well plate with a density of 10^5 cells/well and then cultured in 5% CO_2 atmosphere at 37°C. After 24 hours of incubation, culture medium was replaced and cultured with various Cur formulations at Cur concentration of 20 μg/mL, respectively. Cells incubated with PBS were used as blank control. Cells in new medium were incubated for 8 hours in 5% CO_2 atmosphere at 37°C, after washing three times with cold PBS, cells were harvested for quantitative analysis by flow cytometer on a FACS calibur (BD Bioscience, New Jersey, USA).

MTT assay

HeLa cells were placed into 96-well plates with a density of 5×10^3 per well. After cultured in Dulbecco's Modified Eagle's Medium supplemented with 10% fetal bovine serum at 37°C in 5% CO_2 for 24 hours, a series concentration of empty micelles (including NCM, CCM, and FA-CCM) and various formulations of Cur (free Cur, NCM-Cur, CCM-Cur, and FA-CCM-Cur) with different dilutions were added to the corresponding plate and incubated for 24 hours. Medium in each well was replaced by 20 μL of MTT solution and further incubated for 4 hours. The optical density (OD) at 570 nm was detected by a microplate enzyme-linked immunosorbent assay reader. Cells treated with PBS were used as control, and cell viability was expressed by $([OD_{treat} - OD_{blank}]/[OD_{control} - OD_{blank}]) \times 100$. All samples are presented as mean ± standard deviation (SD) (n=6).

Tissue distribution and tumor accumulations in vivo

BALB/c nude mice were purchased from Vital River Laboratory Animal Technology Co., Ltd. (Beijing, People's Republic of China). The subcutaneous xenograft model of cervical cancer was established by subcutaneously injecting

10^6 HeLa cells in a 0.2 mL of PBS into the right flank of nude mice. The BALB/c nude mice bearing HeLa tumor model were acclimated at 25°C and 55% of humidity under natural light/dark conditions before the size of tumor satisfied the experimental requirements, and all animal experiments were carried out according to the People's Republic of China national standard (GB/T 16886.6-1997). All animal experiments were approved by the Chinese Academy of Medical Science and Peking Union Medical College.

When the volume of tumor model reached 200 mm^3, nude mice were divided into four groups, including free Cur, NCM-Cur, CCM-Cur, and FA-CCM-Cur group, and they were injected intravenously via tail vein at equivalent Cur dose of 10 mg/kg body weight. The tumor and major organs (heart, liver, spleen, lung, and kidney) were dissected from sacrificed mice at scheduled time (1 hour, 6 hours, 24 hours, and 48 hours), these obtained tissues were examined using Kodak IS in vivo imaging system through the fluorescence of Cur with an excitation wavelength of 465 nm and an emission wavelength of 535 nm.

Statistical analysis

One-way analysis of variance was used for the statistical analysis. $*P<0.05$ and $**P<0.01$ were utilized for statistical significance. All data were shown as mean ± SD.

Results and discussion

Synthesis and characterization of copolymer

The PGDS copolymers were synthesized via reversible addition fragmentation chain transfer polymerization,[35] the synthesis routes are shown in Figure 2A. Chemical structures and compositions of PGDS were determined by ^{1}H NMR. As shown in Figure 3A, the monomer DS had been successfully synthesized. All typical peaks of PEG and DS are shown in Figure 3B. The characteristic peaks of DS appeared at 7.02 ppm (c), 8.12 ppm (d), and 7.65 ppm (a+b), and a library of new signals attributed to the protons of PEG chains was found to be at 3.64 ppm (g+h). The copolymers consisted of 31 DS monomers, which were calculated by ^{1}H NMR. Overall, PGDS copolymers were successfully synthesized.

NCM was prepared via nanoprecipitation method. As shown in Figure 4, the diameter of NCM was ~105.7 nm with a narrow polydispersity index of 0.21. Similarly, the CCM retained a spherical shape and smaller particle size of 91.2 nm with a narrow polydispersity index of 0.23 following a disulfide bond cross-linking.

Characterization of redox sensitivity of CCM

The encapsulation stability of CCM compared with NCM under different pH values was assessed by the change in fluorescence intensity. As shown in Figure 5 A–D, unlike the obvious decline of fluorescence intensity of NCM-NR with increased incubation time, there was no significant difference in CCM-NR, which indicated that the drug loading stability of CCM was significantly better than that of NCM. The rate of dye release of NCM-NR incubated in pH 5.0 buffer was faster than that in pH 7.4 buffer. This may be caused by the deprotonation of the pyridine ring in the hydrophobic part at

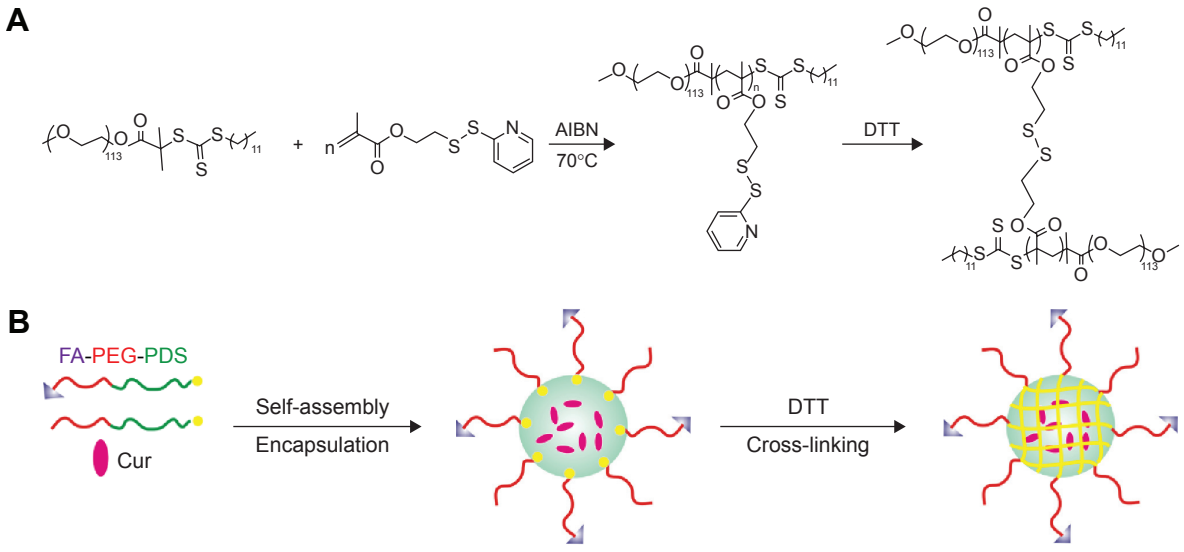

Figure 2 The synthesis route schematic representation of the CCM and FA-CCM-Cur.
Notes: The synthesis route and cross-linking of CCM (**A**). Schematic representation of the preparation and cargos loading method of NCM and FA-CCM (**B**).
Abbreviations: CCM, cross-linked micelle; NCM, noncross-linked micelle; FA, folic acid; FA-PEG, folic acid-polyethylene glycol; PDS, pyridyldisulfide; Cur, curcumin; DTT, dithiothreitol; AIBN, 2,2-azobis (isobutyronitrile).

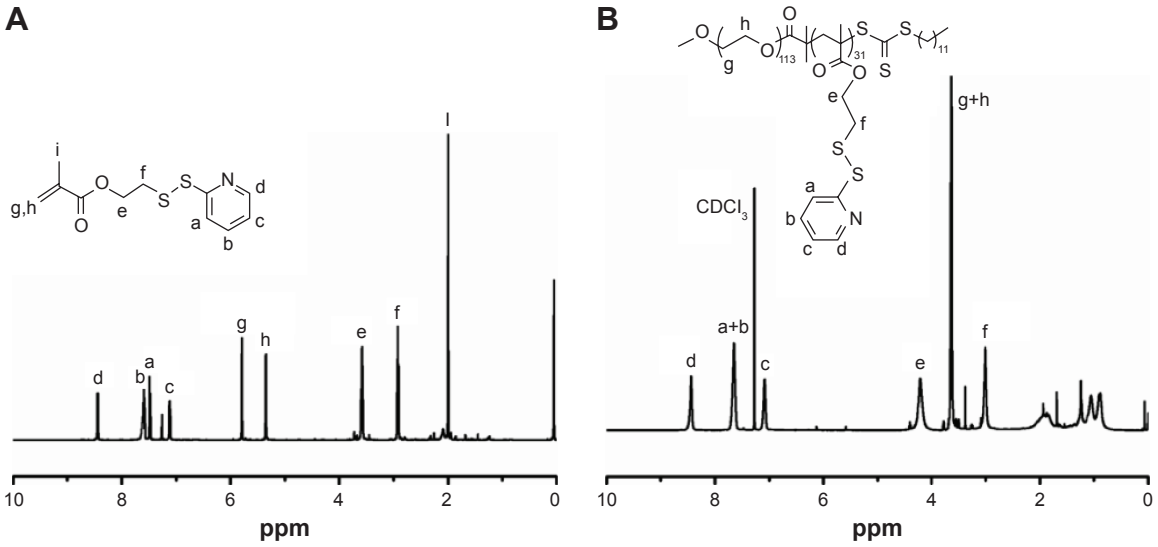

Figure 3 ^{1}H NMR spectrum of DS monomer and PGDS copolymer.
Notes: ^{1}H NMR spectrum of DS monomer (**A**) and PGDS copolymer (**B**) in $CDCl_3$.
Abbreviations: DS, *N*-(2-(2-pyridyl disulde) ethyl methacrylamide; PGDS, mPEG-*b*-PDS.

acid condition,[36,37] which led to expansion of the hydrophobic core and accelerated release of Nile Red.[38] Moreover, when being treated with 10 mM GSH, fluorescence intensity of CCM-NR significantly decreased and ~80% of Nile Red was released after cultured for 24 hours (Figure 5E and F). These results indicated that this CCM could retain higher drug loading stability and achieve targeted drug release in response to high reducibility stimulus.[32,39]

Drug release studies in vitro

The NCM-Cur, CCM-Cur, and FA-CCM-Cur were prepared. The DLC and DLE were determined by ultraviolet–visible spectra, and the size distribution of these micelles was evaluated by dynamic light scattering. As shown in Table 1, the DLC and DLE of the three micelles were ~8% and ~80%, respectively. The particle sizes of them were ~100 nm, which could enable these spherical vehicles to target tumor tissues via enhanced permeability and retention effect.[5,6]

The Cur release profiles from NCM and CCM are shown in Figure 6A and 6B, less Cur was released from CCM than from NCM at pH 7.4, which proved higher loading stability after being cross-linked by disulfide bond. These results may contribute to the reduced drug leakage from CCM during sample storage and blood circulation in vivo.[40] Meanwhile, compared to NCM-Cur, CCM-Cur realized sustained release under the condition of 10 mM GSH,

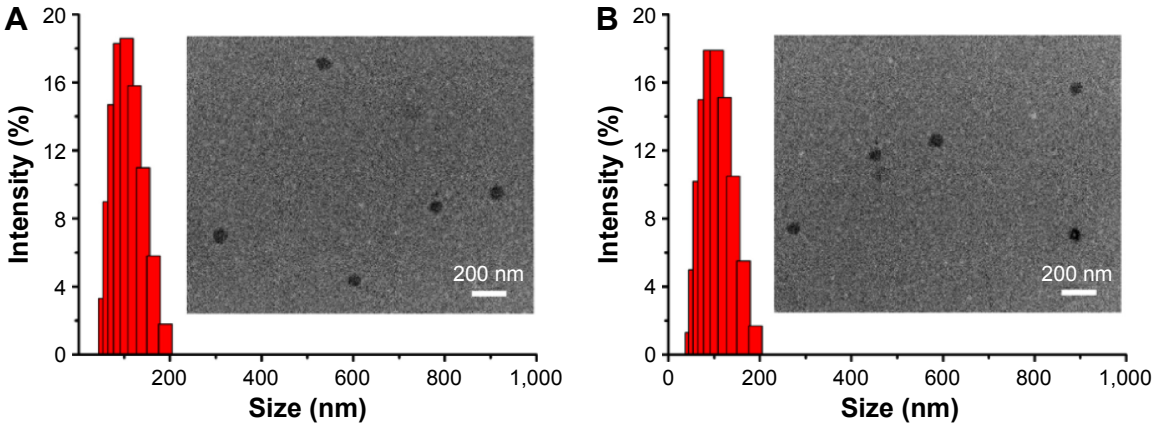

Figure 4 Size distribution and morphology of NCM and CCM.
Notes: Size distribution and morphology of NCM (**A**) and CCM (**B**) measured by DLS and TEM.
Abbreviations: DLS, dynamic light scattering; TEM, transmission electron microscope; NCM, noncross-linked micelle; CCM, cross-linked micelle.

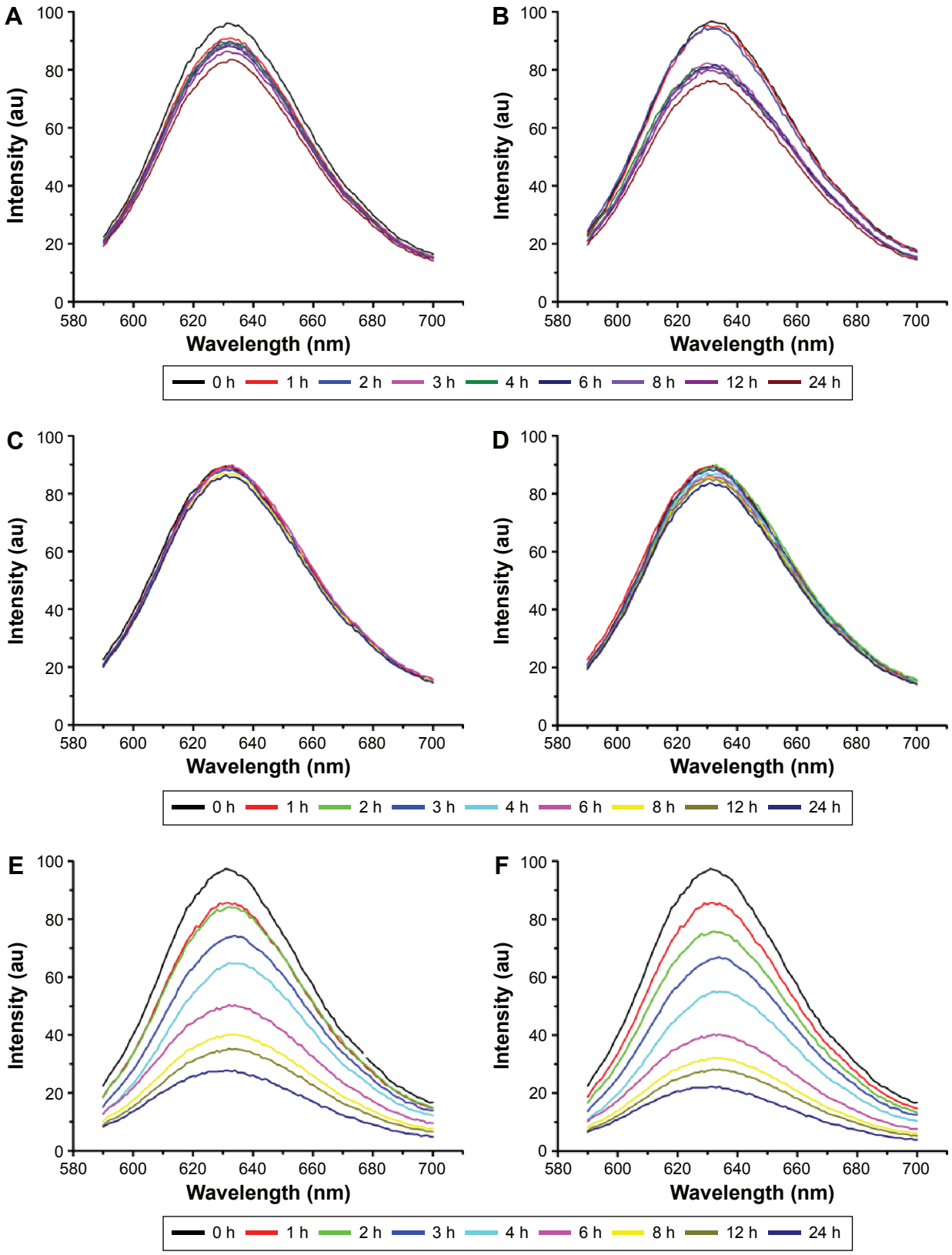

Figure 5 Nile Red release profiles of NCM and CCM at different pH values and reducing environments within 24 hours.
Notes: The release from NCM at neutral pH (**A**) and acidic pH (**B**), the release from CCM at neutral pH (**C**) and acidic pH (**D**), and the release from CCM at neutral pH (**E**) and acidic pH (5.0) (**F**) under 10 mM GSH.
Abbreviations: NCM, noncross-linked micelle; CCM, cross-linked micelle; GSH, glutathione; h, hours.

Table 1 Chemical characteristics of different Cur-loaded micelles

Sample	Size (nm)	PDI	DLC (%)	DLE (%)
NCM-Cur	103±3.2	0.35±0.33	8.25	82.5
CCM-Cur	100±2.6	0.42±0.30	8.35	83.5
FA-CCM-Cur	108±3.5	0.46±0.42	8.31	83.1

Note: Results are expressed as mean ± SD (n=3).
Abbreviations: PDI, polydispersity index; DLC, drug loading content; DLE, drug loading efficiency; NCM, noncross-linked micelle; Cur, curcumin; CCM, core cross-linked micelle; FA, folic acid.

~70%–80% of Cur released within 12 hours of incubation at neutral pH or acidic pH environment (Figure 6A and B). The responsive drug release of CCM-Cur by 10 mM GSH treatment may facilitate the intracellular delivery of loaded molecules and drug accumulation in tumors.[24,31,41] Besides, the different release behaviors of NCM-Cur and CCM-Cur at pH 5.0 was attributed to the pyridine ring of NCM, which would be deprotonated to the acid stimuli and thus accelerated Cur release.

Cellular uptake studies

To investigate the possibility of using these micelles as drug delivery vehicles, cellular uptake studies were performed. As can be seen from Figure 7A, Cur intensity from NCM-Cur was lower than that from CCM-Cur in HeLa cells. This may due to the high encapsulation stability of CCM-Cur in the culture medium, which make more CCM-Cur to be taken up by cells and thus higher fluorescence intensity.[34,42] Moreover, the different release behaviors between NCM-Cur and CCM-Cur, which was endowed by the redox-responsive cross-linkers in the core of CCM-Cur, enabled the CCM-Cur to stably encapsulate and deliver Cur into cells, and then specifically release it in response to the high reducibility in Hela cells.[43] From Figure 7A we can also observe that the Cur released from FA-CCM-Cur was stronger than that from CCM-Cur. As we all know FA receptors are overexpressed on the surface of many tumor cells, such as HeLa cells and human squamous cell carcinoma cell line of the oral cavity (KB cell).[44–48] The surface modification of nanocarriers by FA could effectively enhance their binding ability to FA positive cells via the folate receptor-mediated targeting delivery, as evidenced by the highest fluorescence accumulation in HeLa cells of the FA-CCM-Cur group. Furthermore, the flow cytometry was used for quantitative detection of the cellular uptake. As shown in Figure 7B, similar trends were found as the observations in Figure 7A.

Cell viability studies

To explore the biocompatibility of the blank micelles and the in vitro antitumor ability of Cur-load micelles, we used the MTT assay to observe the viability of HeLa cells. As shown in Figure 8A, all the micelles exhibited no observable cytotoxicity against HeLa cells even if the concentrations were as high as 5 mg/mL. Meanwhile, the cytotoxicity results of different Cur formulations shown in Figure 8B indicated a dose-dependent pattern after incubation for 24 hours. The cell suppression capacity of free Cur was strongest than other three formulations, this was presumably caused by its easy diffusion through the cellular membrane, compared with the delayed release of Cur from the micelles inside the cells.[49,50] NCM-Cur group showed highest cell viability, which can be

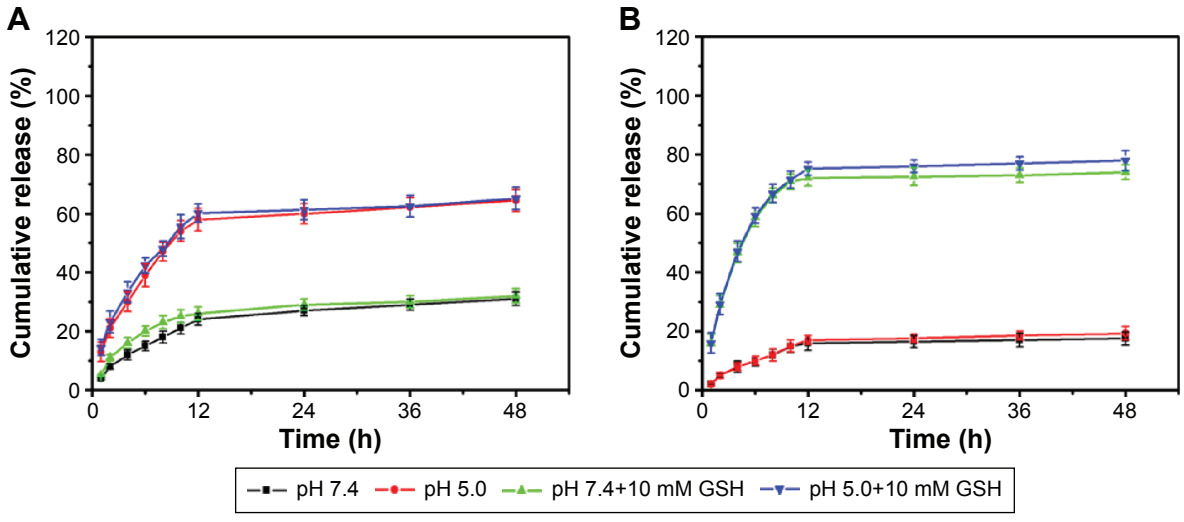

Figure 6 Cur release profiles of NCM and CCM at different conditions.
Notes: Cur release profiles of NCM (**A**) and CCM (**B**) at different pH values with or without GSH treated. Data reported are the mean ± SD for triplicate samples.
Abbreviations: NCM, noncross-linked micelle; CCM, cross-linked micelle; GSH, glutathione; h, hours.

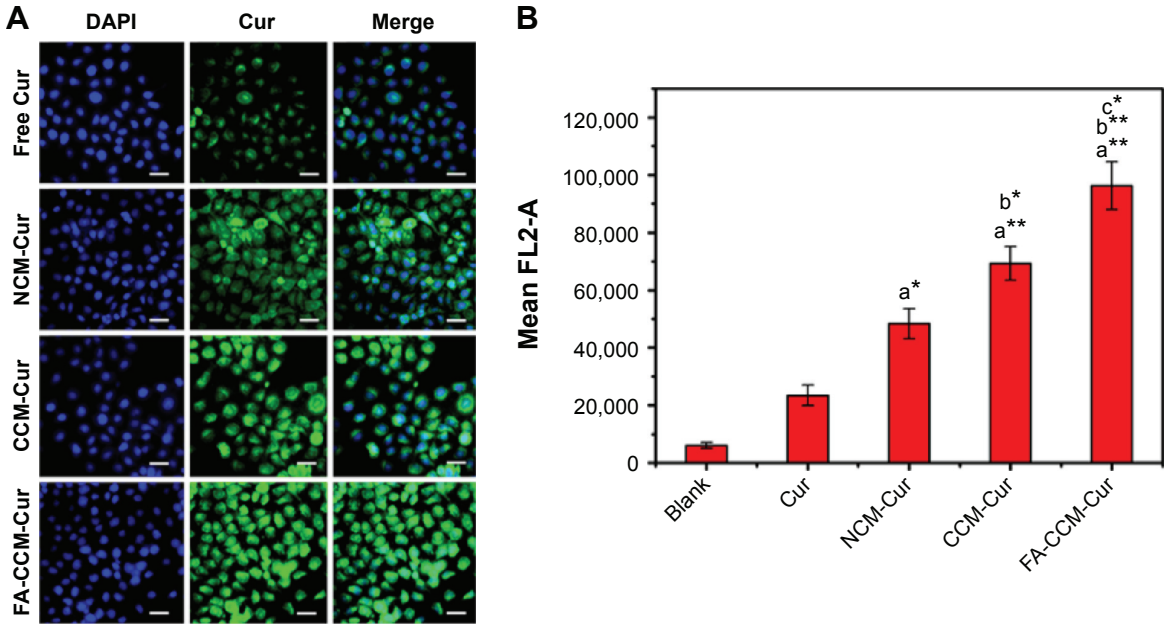

Figure 7 Cellular uptake of different Cur formulations in HeLa cells after incubation for 8 hours.
Notes: (**A**) Cellular uptake of different Cur formulations in HeLa cells after incubation for 8 hours (blue and green represented the cell nucleus and Cur, respectively). Scale bar =25 μm. (**B**) Quantitative analysis of cell uptake by HeLa cells treated with free Cur or Cur-loaded micelles after treatment for 8 hours. (*$P<0.05$, **$P<0.01$, a = in comparison with free Cur, b = in comparison with NCM-Cur, and c = in comparison with CCM-Cur).
Abbreviations: Cur, curcumin; NCM, noncross-linked micelle; CCM, cross-linked micelle; DAPI, 4′,6-diamidino-2-phenylindole; FA, folic acid.

explained by insufficient drug diffused out from NCM, resulting in lowest antitumor efficiency.[51] The core cross-linking micelle showed better cell inhibition effect than NCM-Cur, which was mainly attributed to the controlled and sustained release by the responsibility of disulfide to the reducing agents in the cancer cells.[32,33] Furthermore, FA-CCM-Cur enhanced the inhibition of cell proliferation and showed the best antitumor potential in cellular level, which coincided well with the cellular uptake results.

Ex vivo distribution and tumor accumulations

The distribution and tumor accumulations results of various Cur formulations are shown in Figure 9A and B. Free Cur suffered rapid clearance from main organs and little drug accumulated into tumor after injection for 6 hours. The result verified the fact that there was a short half-life and rapid clearance of Cur.[52] Meanwhile, the shortest time of tumor accumulation of NCM-Cur among the three micelle groups

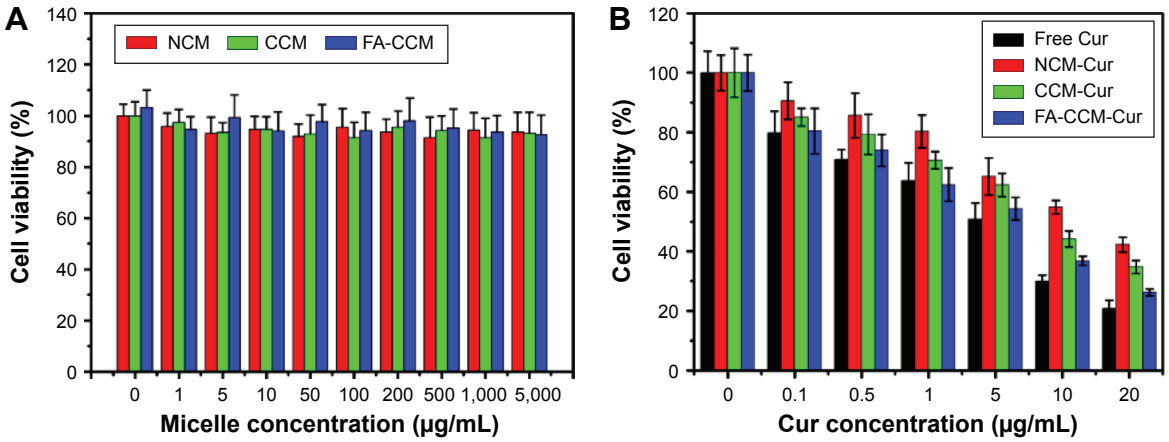

Figure 8 Cell viability of blank micelles and Cur loaded micelles.
Notes: Cell viability of HeLa cells treated with different concentrations of blank micelles (**A**) and different concentrations of Cur-loaded micelles (**B**) after incubation for 24 hours by MTT assay. Values are reported as the mean ± SD (n=6).
Abbreviations: Cur, curcumin; MTT, 3-(4,5-dimethyl-2-thiazolyl)-2,5-diphenyl-2-H-tetrazolium bromide; NCM, noncross-linked micelle; CCM, cross-linked micelle; FA, folic acid.

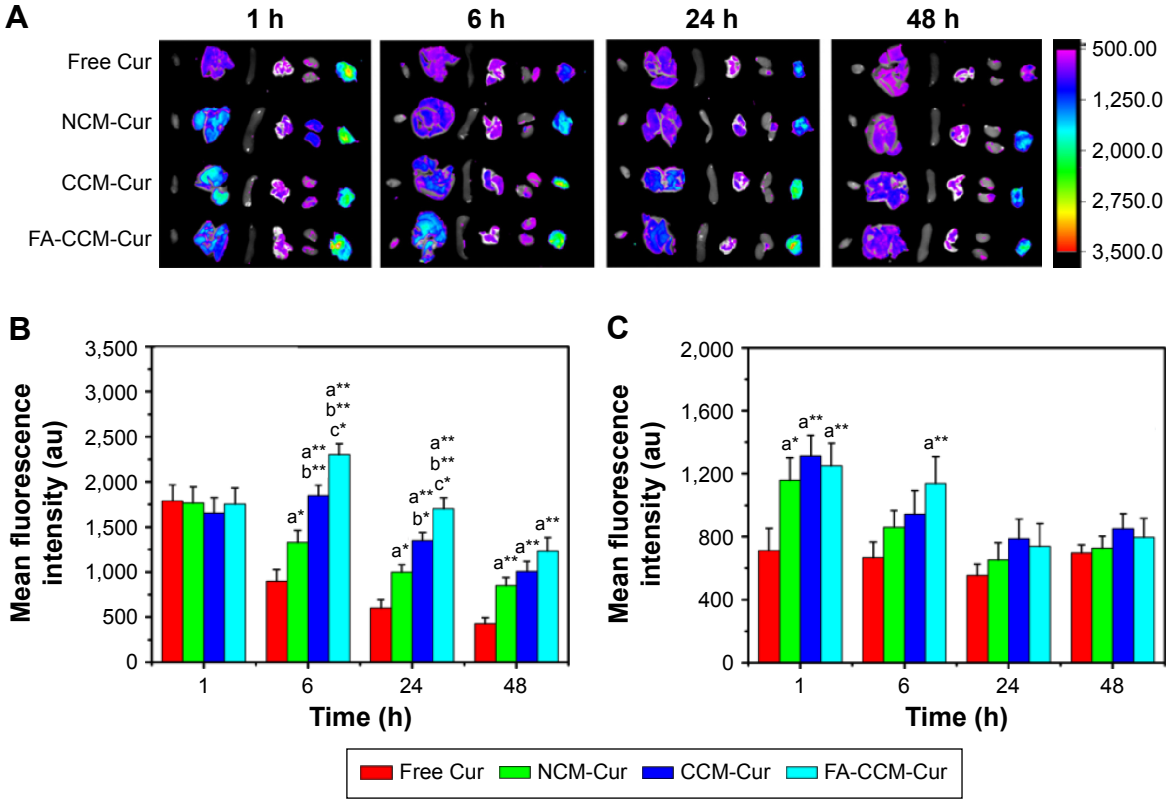

Figure 9 Tissue distribution and tumor accumulations of different Cur formulations.
Notes: Tissue distribution and tumor accumulation images of different Cur formulations (**A**) (from left to right is the heart, liver, spleen, lung, kidney, and tumor, respectively). Quantitative measurement of the Cur intensity in tumor (**B**) and in liver (**C**) within 48 hours (*$P<0.05$, **$P<0.01$, a = in comparison with free Cur, b = in comparison with NCM-Cur, c = in comparison with CCM-Cur) (values are reported as the mean ± SD, n=3).
Abbreviations: Cur, curcumin; MTT, 3-(4,5-dimethyl-2-thiazolyl)-2,5-diphenyl-2-H-tetrazolium bromide; NCM, noncross-linked micelle; CCM, cross-linked micelle; FA, folic acid; h, hours.

may weaken the efficacy of cancer chemotherapy, which was mainly caused by drug leakage in blood circulation or slow passive diffusion into tumor site.[12,38] CCM-Cur showed longer residence time in tumor until 24 hours after injection. This may be resulted from the fact that the CCMs remained intact during the circulation,[38,53] and achieved rapid release in response to the GSH stimulus at the tumor sites. Therefore, FA-CCM-Cur, which combined folate receptor-mediated active targeting drug delivery with the stable drug delivery during circulation endowed by the core cross-linking, showed the highest (at all the time points) and the longest (even 48 hours after injection) Cur accumulation in tumor. Meanwhile, we found that a relatively higher accumulation in the liver was observed compared to that in other organs, which is likely due to the nonspecific accumulation or clearance of nanoparticles by the reticuloendothelial system. Meanwhile, FA-CCM was also dissolved in liver, which was caused by high GSH concentrations in liver. The statistical results of Cur accumulated livers in the three micelles showed no significant differences (Figure 9C).

Conclusion

In summary, we have demonstrated a self-assembled and CCM based on PEG-PDS/FA-PEG-PDS copolymers. With nanosized spherical shapes, CCM/FA-CCM can be used as a safe drug carrier; it showed enhanced drug encapsulation ability and sensitivity of drug release to GSH stimuli. Aided by the FA ligand, FA-CCM-Cur displayed good tumor cell inhibition ability in vitro and stable drug delivery during circulation, and most importantly, it showed high and durable drug accumulation in a tumor. These results suggested that FA-CCM may be a promising vehicle for stable and intelligent tumor drug delivery. Further studies will focus on the in vivo antitumor efficiency and the optimization of the drug dose to obtain the most effective dose with less side effects during the treatment.

Acknowledgments

We acknowledge the financial supports from NSFC (81471727, 51203189, 51303213, and 81371667), Tianjin Science Foundation (13JCZDJC28100), Outstanding Young

Faculty Award of Peking Union Medical College (YR1471), PUMC Youth Fund and the Fundamental Research Funds for the Central Universities (3332015100), and the IRM-CAMS Research Fund (1606 and 1609).

Disclosure

The authors report no conflicts of interest in this work.

References

1. Li J, Kuang Y, Shi J, et al. Enzyme-instructed intracellular molecular self-assembly to boost activity of cisplatin against drug-resistant ovarian cancer cells. *Angew Chem Int Ed Engl*. 2015;127(45):13505–13509.
2. Pu K, Shuhendler AJ, Jokerst JV, et al. Semiconducting polymer nanoparticles as photoacoustic molecular imaging probes in living mice. *Nat Nanotechnol*. 2014;9(3):233–239.
3. Ding D, Mao D, Li K, et al. Precise and long-term tracking of adipose-derived stem cells and their regenerative capacity via superb bright and stable organic nanodots. *ACS Nano*. 2014;8(12):12620–12631.
4. Wang W, Song H, Zhang J, et al. An injectable, thermosensitive and multicompartment hydrogel for simultaneous encapsulation and independent release of a drug cocktail as an effective combination therapy platform. *J Control Release*. 2015;203:57–66.
5. Guo S, Lin CM, Xu Z, Miao L, Wang Y, Huang L. Co-delivery of cisplatin and rapamycin for enhanced anticancer therapy through synergistic effects and microenvironment modulation. *ACS Nano*. 2014;8(5):4996–5009.
6. Wang H, Liu J, Han A, et al. Self-assembly-induced far-red/near-infrared fluorescence light-up for detecting and visualizing specific protein–peptide interactions. *ACS Nano*. 2014;8(2):1475–1484.
7. Talelli M, Barz M, Rijcken CJ, Kiessling F, Hennink WE, Lammers T. Core-crosslinked polymeric micelles: principles, preparation, biomedical applications and clinical translation. *Nano Today*. 2015;10(1):93–117.
8. Wang BL, Shen Y, Zhang Q, et al. Codelivery of curcumin and doxorubicin by MPEG-PCL results in improved efficacy of systemically administered chemotherapy in mice with lung cancer. *Int J Nanomedicine*. 2013;8:3521–3531.
9. Tai W, Mo R, Lu Y, Jiang T, Gu Z. Folding graft copolymer with pendant drug segments for co-delivery of anticancer drugs. *Biomaterials*. 2014;35(25):7194–7203.
10. Rowinsky EK, Donehower RC. Paclitaxel (taxol). *N Engl J Med*. 1995;332(15):1004–1014.
11. Hennenfent KL, Govindan R. Novel formulations of taxanes: a review. Old wine in a new bottle? *Ann Oncol*. 2006;17(5):735–749.
12. Dai J, Lin S, Cheng D, Zou S, Shuai X. Interlayer-crosslinked micelle with partially hydrated core showing reduction and pH dual sensitivity for pinpointed intracellular drug release. *Angew Chem Int Ed Engl*. 2011;50(40):9404–9408.
13. Qi K, Ma Q, Remsen EE, Clark CG Jr, Wooley KL. Determination of the bioavailability of biotin conjugated onto shell cross-linked (SCK) nanoparticles. *J Am Chem Soc*. 2004;126(21):6599–6607.
14. Ma Q, Remsen EE, Kowalewski T, Wooley KL. Two-dimensional, shell-cross-linked nanoparticle arrays. *J Am Chem Soc*. 2001;123(19):4627–4628.
15. Read ES, Armes SP. Recent advances in shell cross-linked micelles. *Chem Commun*. 2007;(29):3021–3035.
16. Pilon LN, Armes SP, Findlay P, Rannard SP. Synthesis and characterization of shell cross-linked micelles with hydroxy-functional coronas: a pragmatic alternative to dendrimers? *Langmuir*. 2005;21(9):3808–3813.
17. Liu S, Armes SP. The facile one-pot synthesis of shell cross-linked micelles in aqueous solution at high solids. *J Am Chem Soc*. 2001;123(40):9910–9911.
18. Lee SJ, Min KH, Lee HJ, et al. Ketal cross-linked poly (ethylene glycol)-poly (amino acid)s copolymer micelles for efficient intracellular delivery of doxorubicin. *Biomacromolecules*. 2011;12(4):1224–1233.
19. Dai J, Li Q, Liu W, et al. Synthesis and characterization of cell-microenvironment-sensitive leakage-free gold-shell nanoparticles with the template of interlayer-crosslinked micelles. *Chem Commun*. 2015;51(47):9682–9685.
20. Noh I, Kim HO, Choi J, et al. Co-delivery of paclitaxel and gemcitabine via CD44-targeting nanocarriers as a prodrug with synergistic antitumor activity against human biliary cancer. *Biomaterials*. 2015;53:763–774.
21. Lv S, Tang Z, Li M, et al. Co-delivery of doxorubicin and paclitaxel by PEG-polypeptide nanovehicle for the treatment of non-small cell lung cancer. *Biomaterials*. 2014;35(23):6118–6129.
22. Sasaki Y, Akiyoshi K. Nanogel engineering for new nanobiomaterials: from chaperoning engineering to biomedical applications. *Chem Rec*. 2010;10(6):366–376.
23. Chan Y, Wong T, Byrne F, Kavallaris M, Bulmus V. Acid-labile core cross-linked micelles for pH-triggered release of antitumor drugs. *Biomacromolecules*. 2008;9(7):1826–1836.
24. Eckmann DM, Composto RJ, Tsourkas A, Muzykantov VR. Nanogel carrier design for targeted drug delivery. *J Mater Chem B Mater Biol Med*. 2014;2(46):8085–8097.
25. Yue Y, Eun JS, Lee MK, Seo SY. Synthesis and characterization of G5 PAMAM dendrimer containing daunorubicin for targeting cancer cells. *Arch Pharm Res*. 2012;35(2):343–349.
26. Gao F, Li L, Liu T, et al. Doxorubicin loaded silica nanorattles actively seek tumors with improved anti-tumor effects. *Nanoscale*. 2012;4(11):3365–3372.
27. Zhao P, Wang H, Yu M, et al. Paclitaxel loaded folic acid targeted nanoparticles of mixed lipid-shell and polymer-core: in vitro and in vivo evaluation. *Eur J Pharm Biopharm*. 2012;81(2):248–256.
28. Wang S, Low PS. Folate-mediated targeting of antineoplastic drugs, imaging agents, and nucleic acids to cancer cells. *J Control Release*. 1998;53(1):39–48.
29. Petros RA, DeSimone JM. Strategies in the design of nanoparticles for therapeutic applications. *Nat Rev Drug Discov*. 2010;9(8):615–627.
30. Ryu JH, Jiwpanich S, Chacko R, Bickerton S, Thayumanavan S. Surface-functionalizable polymer nanogels with facile hydrophobic guest encapsulation capabilities. *J Am Chem Soc*. 2010;132(24):8246–8247.
31. Ryu JH, Chacko RT, Jiwpanich S, Bickerton S, Babu RP, Thayumanavan S. Self-cross-linked polymer nanogels: a versatile nanoscopic drug delivery platform. *J Am Chem Soc*. 2010;132(48):17227–17235.
32. Xing T, Lai B, Ye X, Yan L. Disulfide core cross-linked PEGylated polypeptide nanogel prepared by a one-step ring opening copolymerization of N-carboxyanhydrides for drug delivery. *Macromol Biosci*. 2011;11(7):962–969.
33. Koo AN, Lee HJ, Kim SE, et al. Disulfide-cross-linked PEG-poly (amino acid) s copolymer micelles for glutathione-mediated intracellular drug delivery. *Chem Commun*. 2008;(48):6570–6572.
34. Huang P, Liu J, Wang W, et al. Zwitterionic nanoparticles constructed with well-defined reduction-responsive shell and pH-sensitive core for "spatiotemporally pinpointed" drug delivery. *ACS Appl Mater Interfaces*. 2014;6(16):14631–14643.
35. Zhao J, Wang H, Liu J, et al. Comb-like amphiphilic copolymers bearing acetal-functionalized backbones with the ability of acid-triggered hydrophobic-to-hydrophilic transition as effective nanocarriers for intracellular release of curcumin. *Biomacromolecules*. 2013;14(11):3973–3984.
36. Vinogradov SV, Bronich TK, Kabanov AV. Nanosized cationic hydrogels for drug delivery: preparation, properties and interactions with cells. *Adv Drug Deliv Rev*. 2002;54(1):135–147.
37. Koehn SK, Tran NL, Gronert S, Wu W. The stability of aryl carbanions derived from pyridine N-oxide: the role of resonance in stabilizing aryl anions. *J Am Chem Soc*. 2009;132(1):390–395.

38. Li Y, Xiao K, Luo J, et al. Well-defined, reversible disulfide cross-linked micelles for on-demand paclitaxel delivery. *Biomaterials*. 2011; 32(27):6633–6645.
39. Jiwpanich S, Ryu JH, Bickerton S, Thayumanavan S. Noncovalent encapsulation stabilities in supramolecular nanoassemblies. *J Am Chem Soc*. 2010;132(31):10683–10685.
40. Kabanov AV, Batrakova EV, Alakhov VY. Pluronic® block copolymers as novel polymer therapeutics for drug and gene delivery. *J Control Release*. 2002;82(2):189–212.
41. Ma B, Wang X, Wu C, Chang J. Crosslinking strategies for preparation of extracellular matrix-derived cardiovascular scaffolds. *Regen Biomater*. 2014;1(1):81–89.
42. Deng H, Zhang Y, Wang X, et al. Balancing the stability and drug release of polymer micelles by the coordination of dual-sensitive cleavable bonds in cross-linked core. *Acta Biomater*. 2015;11:126–136.
43. Fan W, Wang Y, Dai X, Shi L, Mckinley D, Tan C. Reduction-responsive crosslinked micellar nanoassemblies for tumor-targeted drug delivery. *Pharm Res*. 2015;32(4):1325–1340.
44. Yoo HS, Park TG. Folate receptor targeted biodegradable polymeric doxorubicin micelles. *J Control Release*. 2004;96(2):273–283.
45. Lee SJ, Shim YH, Oh JS, Jeong YI, Park IK, Lee HC. Folic-acid-conjugated pullulan/poly (DL-lactide-co-glycolide) graft copolymer nanoparticles for folate-receptor-mediated drug delivery. *Nanoscale Res Lett*. 2015;10(1):1–11.
46. Jie Z, Lei L, Lina Z, Jilie K, Baohong L. Folate functionalized mesoporous carbon nanospheres as nanocarrier for targetted delivery and controlled release of doxorubicin to HeLa cells. *Acta Chim Sin*. 2013; 71(1):69–74.
47. Venkatasubbu GD, Ramasamy S, Ramakrishnan V, Kumar V. Folate targeted PEGylated titanium dioxide nanoparticles as a nanocarrier for targeted paclitaxel drug delivery. *Adv Powder Technol*. 2013;24(6): 947–954.
48. Misra R, Upadhyay M, Perumal V, Mohanty S. In vitro control release, cytotoxicity assessment and cellular uptake of methotrexate loaded liquid-crystalline folate nanocarrier. *Biomed Pharmacother*. 2015;69: 102–110.
49. Yu Y, Chen CK, Law WC, et al. Polylactide-graft-doxorubicin nanoparticles with precisely controlled drug loading for pH-triggered drug delivery. *Biomacromolecules*. 2014;15(2):524–532.
50. Prabaharan M, Grailer JJ, Pilla S, Steeber DA, Gong S. Amphiphilic multi-arm-block copolymer conjugated with doxorubicin via pH-sensitive hydrazone bond for tumor-targeted drug delivery. *Biomaterials*. 2009;30(29):5757–5766.
51. Savić R, Azzam T, Eisenberg A, Maysinger D. Assessment of the integrity of poly (caprolactone)-b-poly (ethylene oxide) micelles under biological conditions: a fluorogenic-based approach. *Langmuir*. 2006; 22(8):3570–3578.
52. Ramalingam P, Ko YT. A validated LC-MS/MS method for quantitative analysis of curcumin in mouse plasma and brain tissue and its application in pharmacokinetic and brain distribution studies. *J Chromatogr B Analyt Technol Biomed Life Sci*. 2014;969:101–108.
53. Li Y, Xiao K, Zhu W, Deng W, Lam KS. Stimuli-responsive cross-linked micelles for on-demand drug delivery against cancers. *Adv Drug Deliv Rev*. 2014;66:58–73.